Journal of Applied Fluid Mechanics, Vol. 8, No. 4, pp. 539- 547, 2015.
Available online at www.jafmonline.net, ISSN 1735-3572, EISSN 1735-3645.
DOI: 10.18869/acadpub.jafm.67.222.19361

Pressure Corrections for the Potential Flow Analysis of Electrohydrodynamic Kelvin-Helmholtz Instability

M. Kumar Awasthi[1†] and V. Kumar[2]

[1]*Department of Mathematics, University of Petroleum and Energy Studies, Dehradun, 248007, India*
[2]*Department of Mathematics, University of Petroleum and Energy Studies, Dehradun, 248007, India*

†*Corresponding Author Email: mukeshiitr.kumar@gmail.com*

(Received March 30, 2012; accepted August 01, 2014)

ABSTRACT

The present paper deals with the study of the pressure corrections to the viscous potential flow analysis of Kelvin-Helmholtz instability with tangential electric field at the interface of two viscous fluids. Viscosity enters through normal stress balance in the viscous potential flow theory and tangential stresses for two fluids are not continuous at the interface. Here we have considered viscous pressure in the normal stress balance along with the irrotational pressure and it is assumed that the addition of this viscous pressure will resolve the discontinuity between the tangential stresses and the tangential velocities at the interface of two fluids. The viscous pressure is derived by mechanical energy balance equation and this pressure correction applied to compute the growth rate of electrohydrodynamic Kelvin-Helmholtz instability. A dispersion relation is obtained and stability criterion is given in the terms of critical value of relative velocity. It has been observed that the inclusion of irrotational shearing stresses have stabilizing effect on the stability of the system.

Keywords: Pressure correction; Viscous potential flow; Electrohydrodynamic stability; Incompressible fluid; Interfacial flows.

1. INTRODUCTION

Kelvin-Helmholtz instability arises when two fluid layers of different physical properties are superposed one over other and are moving parallel to each other with a horizontal relative velocity [Chandrasekhar, Drazin and Reid]. The Kelvin-Helmholtz instability occurs in various situations such as wind blowing over the ocean, meteor is entering the earth atmosphere and in oil exploration industry etc.

In viscous potential flow, viscous term in the Navier-stokes equation is identically zero when the vorticity is zero but the viscous stresses are not zero (Joseph and Liao 1994). Tangential stresses are not considered in viscous potential flow theory and viscosity enters through normal stress balance. In this theory no-slip condition at the boundary is not enforced so that two dimensional solutions satisfy three dimensional solutions. Joseph *et al.* (1999) have studied viscous potential flow analysis of Rayleigh-Taylor instability and observed that the length of the most dangerous wave increases strongly with viscosity. The viscous potential flow analysis of Kelvin-Helmholtz instability at the plane geometry is studied by Joseph and Funada (2001). They have observed that the stability criterion for viscous potential flow is given by the critical value of relative velocity. Awasthi and Agrawal (2011) have studied the viscous potential flow analysis of Kelvin-Helmholtz instability of cylindrical interface and observed that the viscous potential flow solution is more stable than inviscid potential flow solution.

As the electric field plays an important role in many practical problems of chemical engineering and other related fields, there is increasing interests in the study of electrohydrodynamic instability. The nonlinear Kelvin-Helmholtz instability in the presence of normal electric field with surface charge has been investigated by Mohamed and El-Shehaway (1989). Mohamed *et al.* (1994) studied the nonlinear electrohydrodynamic Kelvin-Helmholtz instability of inviscid fluids with heat and mass transfer in presence of a tangential electric field and observed that heat and mass transfer plays dual role in the stability criterion in contrast with linear analysis. The viscous potential flow analysis of Kelvin-Helmholtz instability in the presence of tangential electric field when there is heat and mass transfer across the interface has been studied by Asthana and Agrawal (2010).They have observed that the tangential electric field has stabilizing effect on the stability of the system.

Viscous correction for the viscous potential flow (VPF) is called VCVPF. It is also an irrotational flow which differs from VPF only by additional viscous pressure. Wang *et al.* (2005) have given the idea that the effect of the shearing stresses can included in the system by adding viscous pressure in the normal stress balance along with irrotational pressure. Wang *et al.* (2005) have considered the contribution made by shearing stresses for capillary instability in which one fluid is taken as viscous and other fluid is a gas of negligible density and viscosity. They included the viscous pressure in the normal stress balance at the free surface and showed that the growth rates computed using VCVPF is almost same as computed for exact solution. Wang *et al.* (2005) studied the viscous contribution to the pressure for potential flow analysis of capillary instability of two viscous fluids; they found that the viscous correction of the pressure leads to an excellent approximation of the exact solution, uniform in the wave number, when one of the fluids is gas.

Recently, Awasthi and Agrawal (2011) have studied the viscous contribution to the pressure for the potential flow analysis of Kelvin-Helmholtz instability in the presence of tangential magnetic field and observed that the inclusion of irrotational shearing stresses stabilize the system. The viscous contribution to the pressure for the potential flow analysis of capillary instability in the presence of axial electric field has been studied by Awasthi and Agrawal (2011). They have observed that the axial electric field and irrotational shearing stresses both have stabilizing effect on the stability of the system.

The objective of the present work is to include the effect of shearing stresses in the potential flow analysis of the Kelvin-Helmholtz instability of two viscous fluids in the presence of electric field acting in the direction of streaming. Both fluids are taken as dielectric, viscous with different kinematic viscosities, different permittivity and having relative horizontal velocity. In the viscous potential flow analysis the effect of irrotational shearing stresses is completely neglected. Here we have considered viscous pressure in the normal stress balance along with irrotational pressure and this viscous pressure will include the effect of shearing stresses in the system. The formulation for the pressure correction is derived and it is used to compute growth rates for Kelvin-Helmholtz instability with electric field acting in the direction of streaming. It has observed that the effect of irrotational shear stresses stabilize the system.

2. PROBLEM FORMULATION

Consider a system of two incompressible, viscous and dielectric fluid layers of finite thickness whose undisturbed interface is at $y = 0$ as demonstrated in

Fig.1. After disturbance the interface is given by:

$$F(x, y, t) = y - \eta(x, t) = 0 \tag{1}$$

The unit outward normal to the first order term is given by:

$$\boldsymbol{n} = -\frac{\partial \eta}{\partial x}\mathbf{e}_x + \mathbf{e}_y \tag{2}$$

In the undisturbed state, lower fluid of density $\rho^{(1)}$, viscosity $\mu^{(1)}$ and dielectric constant $\varepsilon^{(1)}$ occupies the region $-h_1 < y < 0$ and upper fluid of density $\rho^{(2)}$, viscosity $\mu^{(2)}$ and dielectric constant $\varepsilon^{(2)}$ occupies the region $0 < y < h_2$. The bounding surfaces $y = -h_1$ and $y = h_2$ are considered to be rigid. The lower and upper fluids have uniform flow $(U_1, 0)$ and $(U_2, 0)$ respectively. Both fluids are assumed to be incompressible and irrotational.

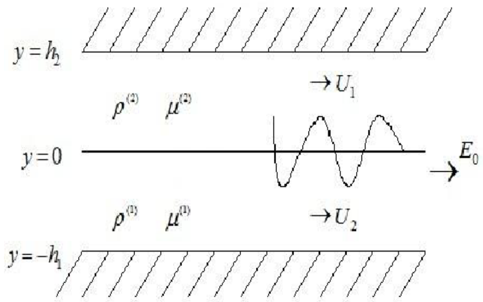

Fig. 1. The equilibrium configuration of the fluid system.

In each fluid layer velocity is given by the potential function $\phi(x, y, t)$ and the potential function satisfies Laplace equation, so

$$\nabla^2 \phi^{(j)} = 0 \qquad (j = 1, 2) \tag{3}$$

where

$$\nabla^2 = \frac{\partial^2}{\partial x^2} + \frac{\partial^2}{\partial y^2}$$

The two fluids are subjected to external electric field E_0 along x-axis *i.e.*

$$\boldsymbol{E_j} = E_0 \boldsymbol{e}_x \qquad \text{for} \quad (j = 1, 2) \tag{4}$$

In this analysis, it is assumed that quasi static approximation is valid for the problem; hence the electric field can be derived from electric scalar potential function $\psi(x, y, t)$ such that

$$\boldsymbol{E_j} = E_0 \boldsymbol{e}_x - \nabla \psi^{(j)} \qquad \text{for} \quad (j = 1, 2) \tag{5}$$

Gauss's law requires that the electric potential also satisfies Laplace equation i.e.

$$\nabla^2 \psi^{(j)} = 0 \qquad (j = 1, 2) \tag{6}$$

In the initial state we assume,

$$\phi_0^{(j)} = U_j x \qquad (j = 1, 2) \tag{7}$$

As per the kinematic condition, every particle on the interface will remain on the interface; we get the following boundary conditions:

$$\frac{\partial \eta}{\partial t}+U_1\frac{\partial \eta}{\partial x}=\frac{\partial \phi^{(1)}}{\partial y} \tag{8}$$

$$\frac{\partial \eta}{\partial t}+U_2\frac{\partial \eta}{\partial x}=\frac{\partial \phi^{(2)}}{\partial y} \tag{9}$$

Conditions on the wall are given by:

$$\frac{\partial \phi^{(1)}}{\partial y}=0 \quad \text{at} \quad y=-h_1 \tag{10}$$

$$\frac{\partial \phi^{(2)}}{\partial y}=0 \quad \text{at} \quad y=h_2 \tag{11}$$

$$\frac{\partial \psi^{(1)}}{\partial y}=0 \quad \text{at} \quad y=-h_1 \tag{12}$$

$$\frac{\partial \psi^{(2)}}{\partial y}=0 \quad \text{at} \quad y=h_2 \tag{13}$$

The tangential component of the electric field must be continuous across the interface i.e.

$$\mathbf{n}\wedge[\mathbf{E}]=0 \quad \text{or} \quad \left[\frac{\partial \psi}{\partial x}\right]+\frac{\partial \eta}{\partial x}\left[\frac{\partial \psi}{\partial y}\right]=0 \tag{14}$$

where $[x]=x^{(2)}-x^{(1)}$ in which superscripts refers to upper and lower fluid respectively.

The normal component of electric displacement must be continuous across the interface i.e.

$$\mathbf{n}\cdot[\varepsilon\mathbf{E}]=0 \quad \text{or} \quad \mathrm{E}_0\frac{\partial \eta}{\partial x}[\varepsilon]-\frac{\partial \eta}{\partial x}\left[\varepsilon\frac{\partial \psi}{\partial x}\right]+\left[\frac{\partial \psi}{\partial y}\right]=0 \tag{15}$$

The interfacial condition for conservation of momentum at the interface is given by:

$$\begin{aligned}&P_2-P_1-2\mu^{(2)}\mathbf{n}\cdot\nabla\otimes\nabla\phi^{(2)}\cdot\mathbf{n}+2\mu^{(1)}\mathbf{n}\cdot\nabla\\&\otimes\nabla\phi^{(1)}\cdot\mathbf{n}-\frac{1}{2}\left[\varepsilon(E_n^2-E_t^2)\right]=-\sigma\nabla\cdot\mathbf{n}\end{aligned} \tag{16}$$

Using normal mode technique to solve the Eqs. (3) for $(j=1,2)$ with the conditions (10) and (11), we get:

$$\phi^{(1)}=A_1\cosh[k(y+h_1)]\exp(ikx-i\omega t)+c.c. \tag{17}$$

$$\phi^{(2)}=A_2\cosh[k(y-h_2)]\exp(ikx-i\omega t)+c.c. \tag{18}$$

Similarly solving the Eqs. (6) for $(j=1,2)$ with conditions (12) and (13), we get:

$$\psi^{(1)}=B_1\cosh[k(y+h_1)]\exp(ikx-i\omega t)+c.c. \tag{19}$$

$$\psi^{(2)}=B_2\cosh[k(y-h_2)]\exp(ikx-i\omega t)+c.c. \tag{20}$$

Let the interface elevation is given by:

$$\eta=A_0\exp(ikx-i\omega t)+c.c \tag{21}$$

where A_0, A_1, A_2, B_1 and B_2 denotes complex amplitudes and c.c. stands for the complex conjugate of the preceding expression, ω is the complex growth rate and $k>0$ denotes the wave number. Eqs. (17), (18), (19) and (20) with boundary conditions, we get:

$$\phi^{(1)}=\frac{1}{k}(ikU_1-i\omega)A_0\frac{\cosh[k(y+h_1)]}{\sinh kh_1}\exp(ikx-i\omega t)+c.c. \tag{22}$$

$$\phi^{(2)}=-\frac{1}{k}(ikU_2-i\omega)A_0\frac{\cosh[k(y-h_2)]}{\sinh kh_2}\exp(ikx-i\omega t)+c.c. \tag{23}$$

$$\psi^{(1)}=\frac{iE_0(\varepsilon^{(2)}-\varepsilon^{(1)})}{(\varepsilon^{(2)}\tanh(kh_2)+\varepsilon^{(1)}\tanh(kh_1))}A_0\frac{\cosh[k(y+h_1)]}{\cosh kh_1}\exp(ikx-i\omega t)+c.c. \tag{24}$$

$$\psi^{(2)}=\frac{iE_0(\varepsilon^{(2)}-\varepsilon^{(1)})}{(\varepsilon^{(2)}\tanh(kh_2)+\varepsilon^{(1)}\tanh(kh_1))}A_0\frac{\cosh[k(y-h_2)]}{\cosh kh_2}\exp(ikx-i\omega t)+c.c. \tag{25}$$

3. PRESSURE CORRECTION FOR VISCOUS POTENTIAL FLOW

The effect of irrotational shearing stresses have been included in the viscous potential flow analysis of electrohydrodynamic Kelvin-Helmholtz instability taking viscous pressure into the normal stress balance along with the irrotational pressure. The mechanical energy equation has been used for the derivation of the pressure correction.

Let $\boldsymbol{n_1}=\boldsymbol{e}_y$ be the unit outward normal at the interface for the upper fluid and $\boldsymbol{n}_2=-\boldsymbol{n}_1$ is the unit outward normal for the lower fluid; let $\boldsymbol{t}=\boldsymbol{e}_x$ be the unit tangent vector .We use the subscript 'v' for viscous and 'i' for irrotational. The normal and shear parts of the viscous stress are represented by τ^n and τ^s respectively.

The Mechanical energy equations for upper and lower fluids are respectively:

$$\frac{d}{dt}\int_{V_2}\frac{\rho^{(2)}}{2}|\mathbf{u}_2|^2dV=\int_{V_2}\rho^{(2)}g\mathbf{u}_2dV+\int_A[\mathbf{u}_2\cdot\mathbf{T}\cdot\mathbf{n}_2]dA-\int_{V_2}2\mu^{(2)}\mathbf{D}_2:\mathbf{D}_2\,dV$$

$$= \int_{V_2} \rho^{(2)} g \mathbf{u}_2 dV - \int_{V_2} 2\mu^{(2)} \mathbf{D}_2 : \mathbf{D}_2 \, dV$$
$$+ \int_A \left[\mathbf{u}_2 \cdot \mathbf{n}_1 (-p_2^i + \tau_2^n) + \mathbf{u}_2 \cdot \mathbf{t} \; \tau_2^s \right] dA \quad (26)$$

$$\frac{d}{dt} \int_{V_1} \frac{\rho^{(1)}}{2} \left| \mathbf{u}_1 \right|^2 dV$$
$$= \int_{V_1} \rho^{(1)} g \mathbf{u}_1 dV + \int_A \left[\mathbf{u}_1 \cdot \mathbf{T} \cdot \mathbf{n}_1 \right] dA - \int_{V_1} 2\mu^{(1)} \mathbf{D}_1 : \mathbf{D}_1 \, dV$$
$$= \int_{V_1} \rho^{(1)} g \mathbf{u}_1 dV - \int_{V_1} 2\mu^{(1)} \mathbf{D}_1 : \mathbf{D}_1 \, dV$$
$$+ \int_A \left[\mathbf{u}_1 \cdot \mathbf{n}_1 (-p_1^i + \tau_1^n) + \mathbf{u}_1 \cdot \mathbf{t} \; \tau_1^s \right] dA \quad (27)$$

with continuity of the normal velocity

$$\mathbf{u_2} \cdot \mathbf{n_1} = \mathbf{u_1} \cdot \mathbf{n_1} = u_n$$

Sum of (27) and (28) can be written as,

$$\frac{d}{dt} \int_{V_2} \frac{\rho^{(2)}}{2} \left| \mathbf{u}_2 \right|^2 dV + \frac{d}{dt} \int_{V_1} \frac{\rho^{(1)}}{2} \left| \mathbf{u}_1 \right|^2 dV =$$
$$\int_{V_2} \rho^{(2)} g \mathbf{u_2} dV + \int_{V_1} \rho^{(1)} g \mathbf{u}_1 dV$$
$$- \int_{V_2} 2\mu^{(2)} \mathbf{D}_2 : \mathbf{D}_2 dV - \int_{V_1} 2\mu^{(1)} \mathbf{D}_1 : \mathbf{D}_1 dV \quad (28)$$
$$+ \int_A \left[u_n (-p_1^i + \tau_1^n + p_2^i - \tau_2^n) + \mathbf{u}_2 \cdot \mathbf{t} \; \tau_2^s - \mathbf{u}_1 \cdot \mathbf{t} \; \tau_1^s \right] dA$$

Here we introduced two pressure corrections p_1^v and p_2^v for lower and upper potential flow respectively. It is assumed that these two pressure corrections will resolve the discontinuity of the shear stress and tangential velocity at the interface, so

$$\tau_1^s = \tau_2^s = \tau^s \qquad \text{and} \qquad \mathbf{u_2} \cdot \mathbf{t} = \mathbf{u_1} \cdot \mathbf{t} = u_s$$

So Eq. (19) becomes

$$\frac{d}{dt} \int_{V_2} \frac{\rho^{(2)}}{2} \left| \mathbf{u}_2 \right|^2 dV + \frac{d}{dt} \int_{V_1} \frac{\rho^{(1)}}{2} \left| \mathbf{u}_1 \right|^2 dV =$$
$$\int_{V_2} \rho^{(2)} g \mathbf{u_2} dV + \int_{V_1} \rho^{(1)} g \mathbf{u}_1 dV$$
$$- \int_{V_2} 2\mu^{(2)} \mathbf{D}_2 : \mathbf{D}_2 dV - \int_{V_1} 2\mu^{(1)} \mathbf{D}_1 : \mathbf{D}_1 dV \quad (29)$$
$$+ \int_A \left[u_n (-p_1^i - p_1^v + \tau_1^n + p_2^i + p_2^v - \tau_2^n) \right] dA$$

The integrands in the volume integrals in (18) and (19) are computed using potential flows. The VCVPF solution resolves the discontinuities of the tangential stresses and tangential velocities.

Comparing Eqs. (28) and (29), we get:

$$\int_A \left[u_n (-p_1^v + p_2^v) \right] dA = \int_A \left[\mathbf{u_1} \cdot \mathbf{t} \tau_1^s - \mathbf{u_2} \cdot \mathbf{t} \tau_2^s \right] dA \quad (30)$$

The governing equation of pressure correction is given by;

$$\nabla^2 p^v = 0 \quad (31)$$

Solving Eq. (31), two pressure correction is obtained as,

$$p_1^v = -(C_k \cosh ky + E_k \sinh ky) \exp[(ikx - i\omega t)] \quad (32)$$

$$p_2^v = -(D_k \cosh ky + F_k \sinh ky) \exp[(ikx - i\omega t)] \quad (33)$$

4. DISPERSION RELATION

The normal stress balance with viscous pressure is given by:

$$P_2^i + P_2^v - P_1^i - P_1^v - 2\mu^{(2)} \mathbf{n} \cdot \nabla \otimes \nabla \phi^{(2)} \cdot \mathbf{n} + 2\mu^{(1)}$$
$$\mathbf{n} \cdot \nabla \otimes \nabla \phi^{(1)} \cdot \mathbf{n} - \frac{1}{2} \left[\varepsilon (E_n^2 - E_t^2) \right] = -\sigma \nabla \cdot \mathbf{n} \quad (34)$$

Using Bernoulli's equation for irrotational pressure and linearizing it, we get:

$$\begin{bmatrix} \rho \left(\dfrac{\partial \phi}{\partial t} + g\eta + \dfrac{\partial \phi}{\partial x} \dfrac{\partial \phi_0}{\partial x} \right) + P^v \\ +2\mu \dfrac{\partial^2 \varphi}{\partial y^2} + \varepsilon E_0 \dfrac{\partial \psi}{\partial x} \end{bmatrix} = -\sigma \frac{\partial^2 \eta}{\partial x^2} \quad (35)$$

From Eq. (31) we get:

$$[C_k - D_k] = \begin{bmatrix} 2\mu_1 A_0 (ikU_1 - i\omega) \coth(kh_1) \\ + 2\mu_2 A_0 (ikU_2 - i\omega) \coth(kh_2) \end{bmatrix} \quad (36)$$

Substituting the values of η, $\phi^{(1)}, \phi^{(2)}, \psi^{(1)}, \psi^{(2)}$ in Eq. (35), we get dispersion relation:

$$D(\omega, k) = a_0 \omega^2 + (a_1 + ib_1)\omega + a_2 + ib_2 = 0 \quad (37)$$

where

$$a_0 = \rho^{(1)} \coth(kh_1) + \rho^{(2)} \coth(kh_2)$$

$$a_1 = -2k(\rho^{(1)} U_1 \coth(kh_1) + \rho^{(2)} U_2 \coth(kh_2))$$

$$b_1 = 4k^2 (\mu^{(1)} \coth(kh_1) + \mu^{(2)} \coth(kh_2))$$

$$a_2 = k^2 (\rho^{(1)} U_1^2 \coth(kh_1) + \rho^{(2)} U_2^2 \coth(kh_2)) - \sigma k^3$$
$$+ (\rho^{(2)} - \rho^{(1)}) gk - \frac{k^2 E_0^2 (\varepsilon^{(2)} - \varepsilon^{(1)})^2}{(\varepsilon^{(2)} \tanh(kh_2) + \varepsilon^{(1)} \tanh(kh_1))}$$

$$b_2 = -4k^3 (\mu^{(1)} U_1 \coth(kh_1) + \mu^{(2)} U_2 \coth(kh_2))$$

Let $\omega = \omega_R + i\omega_I$, and equating the real and imaginary parts (37) will reduce to

$$a_0 (\omega_R^2 - \omega_I^2) + (a_1 \omega_R - b_1 \omega_I) + a_2 = 0 \quad (38)$$

and

$$2a_0\omega_R\omega_I + a_1\omega_I + b_1\omega_R + b_2 = 0 \qquad (39)$$

So

$$\omega_R = -\frac{a_1\omega_I + b_2}{2a_0\omega_I + b_1}$$

Putting this value in Eq. (38), we obtained a quartic equation in ω_R as,

$$A_4\omega_I^4 + A_3\omega_I^3 + A_2\omega_I^2 + A_1\omega_I + A_0 = 0 \qquad (40)$$

where

$$A_4 = -4a_0^3$$

$$A_3 = -8a_0^2 b_1$$

$$A_2 = 4a_0^2 a_2 - 5a_0 b_1^2 - a_0 a_1^2$$

$$A_1 = 4a_0 a_2 b_1 - b_1^3 - a_1^2 b_1$$

$$A_0 = a_0 b_2^2 - a_0 b_1 b_2 + a_2 b_1^2$$

From Eq. (40) we can get the value of maximum growth rate ω_{Im} and corresponding wave number k_m .To get the neutral curves we put $\omega_I(k) = 0$, so Eq. (40) reduces to:

$A_0 = 0$ i.e.

$$a_0 b_2^2 - a_0 b_1 b_2 + a_2 b_1^2 = 0 \qquad (41)$$

Putting the values of $a_0, a_1, a_2, b_1,$ and b_2 in the above equation, we get:

$$-\coth kh_1 \coth kh_2 \begin{bmatrix} (\rho^{(1)}\mu^{(2)^2} \coth kh_2 \\ +\rho^{(2)}\mu^{(1)^2} \coth kh_1) \end{bmatrix} V^2 + \frac{1}{k}\begin{bmatrix} \sigma k^2 + (\rho^{(1)} - \rho^{(2)})g \\ + \dfrac{k^2 E_0^2(\varepsilon^{(2)} - \varepsilon^{(1)})^2}{(\varepsilon^{(2)}\tanh(kh_2) + \varepsilon^{(1)}\tanh(kh_1))} \end{bmatrix} \qquad (42)$$

$$\left[(\mu^{(2)}\coth kh_2 + \mu^{(1)}\coth kh_1)\right]^2 = 0$$

Here V is the relative velocity which is given by:

$$V = U_2 - U_1$$

Let there be no streaming, i.e. $U_2 = 0$ and $U_1 = 0$ so $V = 0$, then from equation (40) we get:

$$\sigma k^2 + \left(\rho^{(1)} - \rho^{(2)}\right)g + \frac{kE_0^2(\varepsilon^{(2)} - \varepsilon^{(1)})^2}{(\varepsilon^{(2)}\tanh(kh_2) + \varepsilon^{(1)}\tanh(kh_1))} = 0 \qquad (43)$$

Let the two fluids are semi-infinite i.e.

$h_1 \to \infty$ and $h_2 \to \infty$ so $\coth kh_1 \to 1$ and $\coth kh_2 \to 1$

In this case Eq. (43) becomes

$$V^2 = \frac{1}{k}\frac{\left[\sigma k^2 + (\rho^{(1)} - \rho^{(2)})g + \dfrac{kE_0^2(\varepsilon^{(2)} - \varepsilon^{(1)})^2}{(\varepsilon^{(2)} + \varepsilon^{(1)})}\right]\left[\mu^{(1)} + \mu^{(2)}\right]^2}{\left[\rho^{(1)}\mu^{(2)^2} + \rho^{(2)}\mu^{(1)^2}\right]} \qquad (44)$$

We can obtain lowest point on the Neutral Curve $V^2(k)$ as,

$$V_c^2(k) = \min_{k \ge 0} V^2(k) = V^2(k_c) \qquad (45)$$

Critical wave length is given by $\lambda_c = 2\pi / k_c$. The flow is unstable when

$$V^2 = (-V^2) \ge V_c^2 \qquad (46)$$

5. Dimensionless Form

$$\hat{k} = kh,\ \hat{h}_2 = \frac{h_2}{h},\ \hat{h}_1 = \frac{h_1}{h} = 1 - \hat{h}_2,\ \hat{E} = E\sqrt{\frac{\varepsilon^{(1)}}{\rho^{(1)}gh}}$$

$$\hat{U}_2 = \frac{U_2}{Q},\ \hat{U}_1 = \frac{U_1}{Q},\ \hat{V} = \hat{U}_2 - \hat{U}_1,\ \hat{\sigma} = \frac{\sigma}{\rho^{(1)}gH^2}$$

$$\hat{\rho} = \frac{\rho^{(2)}}{\rho^{(1)}},\ \hat{\mu} = \frac{\mu^{(2)}}{\mu^{(1)}},\ \hat{\omega} = \frac{\omega h}{Q},\ \theta = \frac{\mu^{(1)}}{\rho^{(1)}HQ},\ \hat{\varepsilon} = \frac{\varepsilon^{(2)}}{\varepsilon^{(1)}}$$

Where $Q = \left[((1-\hat{\rho})gH)/\hat{\rho}\right]^{1/2}$

The dimensionless form of Eq. (37) is given by

$$\left[\coth\hat{k}\hat{h}_1 + \hat{\rho}\coth\hat{k}\hat{h}_2\right]\hat{\omega}^2 + \begin{bmatrix} -2k\left\{\hat{U}_1\coth\hat{k}\hat{h}_1 + \hat{\rho}\hat{U}_2\coth\hat{k}\hat{h}_2\right\} \\ +4ik^2\theta(\coth\hat{k}\hat{h}_1 + \hat{\mu}\coth\hat{k}\hat{h}_2) \end{bmatrix}\hat{\omega} + \begin{bmatrix} k^2(\hat{U}_1^2\coth\hat{k}\hat{h}_1 + \hat{\rho}\hat{U}_2^2\coth\hat{k}\hat{h}_2) \\ -\hat{\rho}\hat{k}\begin{Bmatrix} 1 + \dfrac{\hat{\sigma}\hat{k}^2}{(1-\hat{\rho})} + \dfrac{\hat{k}\hat{E}^2}{(1-\hat{\rho})} \\ \dfrac{(\hat{\varepsilon}-1)^2}{(\tanh(\hat{k}\hat{h}_1) + \hat{\varepsilon}\tanh(\hat{k}\hat{h}_2))} \end{Bmatrix} \\ -4ik^3\theta\left\{\hat{U}_1\coth\hat{k}\hat{h}_1 + \hat{\mu}\hat{U}_2\coth\hat{k}\hat{h}_2\right\} \end{bmatrix} = 0 \qquad (47)$$

The Eq.(42) in dimensionless form may be written as,

$$-\coth\hat{k}\hat{h}_1\coth\hat{k}\hat{h}_2\left[\hat{\rho}\coth\hat{k}\hat{h}_1 + \hat{\mu}^2\coth\hat{k}\hat{h}_2\right]\hat{V}^2 + \frac{\hat{\rho}}{k}\begin{Bmatrix} 1 + \dfrac{\hat{\sigma}\hat{k}^2}{(1-\hat{\rho})} + \dfrac{\hat{k}\hat{E}^2}{(1-\hat{\rho})} \\ \dfrac{(\hat{\varepsilon}-1)^2}{(\tanh(\hat{k}\hat{h}_1) + \hat{\varepsilon}\tanh(\hat{k}\hat{h}_2))} \end{Bmatrix}\times$$

$$\left[\coth\hat{k}\hat{h}_1 + \hat{\mu}\coth\hat{k}\hat{h}_2\right]^2 = 0 \qquad (48)$$

6. RESULTS AND DISCUSSION

The dispersion relation for the linear analysis of electrohydrodynamic Kelvin-Helmholtz instability is quadratic in growth rate and instability occurs due to the positive values of the disturbance growth rate (i.e. $\omega_I > 0$). If ω_I is negative, the perturbation decays with time while if $\omega_I > 0$, the system is unstable as the perturbation grows exponentially with time. The case $\omega_I = 0$ is the marginal stability case. Wang et al. [2005] has pointed out that the approach to add the extra pressure in the normal stress balance does not require the analysis of a boundary layer; it is the approach called the viscous correction of viscous potential flow (VCVPF). It is based on the assumption that the motion is irrotational, the normal stress is computed on the irrotational flow and the extra or corrected pressure can be computed right at the free boundary for the nonzero irrotational shear stresses. This extra viscous pressure is an additional and important viscous contribution to the normal stress.

Following parametric values have been considered for the system of interest containing water in the lower region and air in upper region. Neutral curve for relative velocity divide the plane into the stable region (below the curve) and unstable region (above the curve) while the neutral curves curve for electric field divide the plane into a stable region (above the curve) and an unstable region (below the curve).The effect of various physical parameters on the onset of instability is interpreted from the following Figures.

$\rho^{(1)} = 1.0 gm/cm^3$, $\rho^{(2)} = 0.0012 gm/cm^3$,

$\mu^{(1)} = 0.01 poise$, $\mu^{(1)} = 0.00018 poise$,

$\sigma = 72.3 dyne/cm$, $g = 980 cm/s^2$,

In Fig. 2, the neutral curves for the relative velocity for the water-air system have been drawn with $E_0 = 0$ for various value of upper fluid fraction β. As upper fluid fraction increases, fluid pressure at crest will fall below the equilibrium pressure and as a consequence of this, amplitude of disturbance wave will diminish. It will stabilize the system observed from Fig. 2. The viscous potential flow analysis of Kelvin-Helmholtz instability without electric field has been studied by Funada and Joseph (2001) and they have observed that the upper fluid fraction has stabilizing effect.

In order to observe the effect of electric field on the instability of interface we have plotted Fig. 3. Fig. 3 shows the variation of neutral curves for the relative velocity for water-air system for various values of upper fluid fraction when $E_0 = 10 Volt/cm$. It has been observed that the upper fluid fraction still stabilizes the system even in the presence of tangential electric field. It is clear from the Fig. 2 and 3 that the stable region increases in presence of electric field for same values of other parameters. Hence tangential electric field has stabilizing effect.

Figure 4 represents the neutral curves for the relative velocity at upper fluid fraction β = 0:5 for various values of electric field and observed that the stable region increases as electric field increases. Hence it is concluded that electric field has stabilizing effect. It is clear from the Eq. (48) that in the absence of electric field, the right hand of the Eq. (48) is $\left[(\rho^{(2)} - \rho^{(1)})gk + \sigma k^3\right]$. In the presence of electric field, the term depending on the applied electric field is added in the right hand side of the Eq. (48) and so that critical value of relative velocity increases. This shows that electric field has stabilizing influence. In Fig. 5, variation of the critical value of relative velocity with the ratio of dielectric constants has been shown for different values of applied electric field. Critical value of relative velocity first decreases and then increases. This shows that ratio of dielectric constants of two fluids has dual effect on the stability of the system. At the constant value of the electric field, the most unstable case was found when both the fluids have same dielectric constant i.e. $\hat{\varepsilon} = 1$.

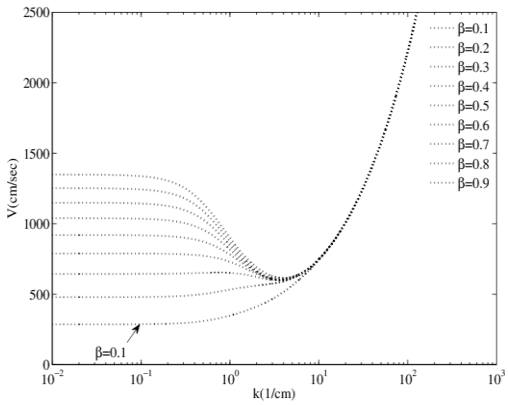

Fig. 2. Neutral curves for the relative velocity for water-air system at $\hat{\rho} = 0.0012, \hat{\mu} = 0.018, E_0 = 0$ for different values of upper different fluid fraction.

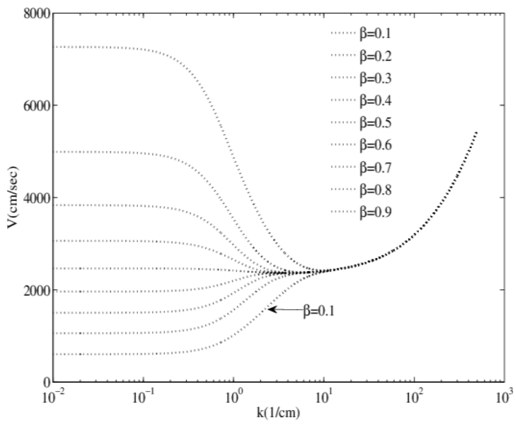

Fig. 3. Neutral curves for the relative velocity for water-air system at $\hat{\rho} = 0.0012, \hat{\mu} = 0.018, E_0 = 10$ for different values of upper different fluid fraction.

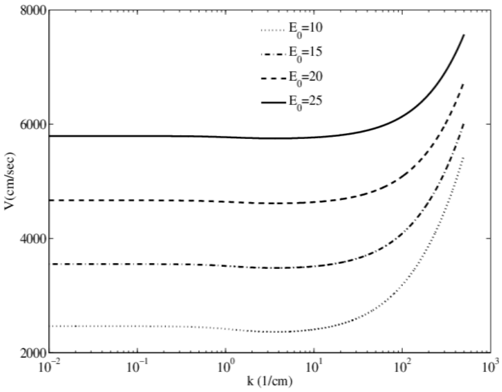

Fig. 4. Neutral curves for the relative velocity for water-air system at $\hat{\rho} = 0.0012, \hat{\mu} = 0.018, \beta = 0.5$ **for different values of electric field intensity** E_0 **.**

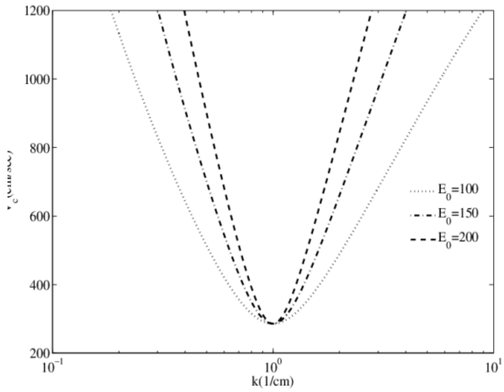

Fig. 5. the critical value of relative velocity for water-air system at $\hat{\rho} = 0.0012, \hat{\mu} = 0.018, \beta = 0.5$ **for different values of electric field intensity** E_0 **.**

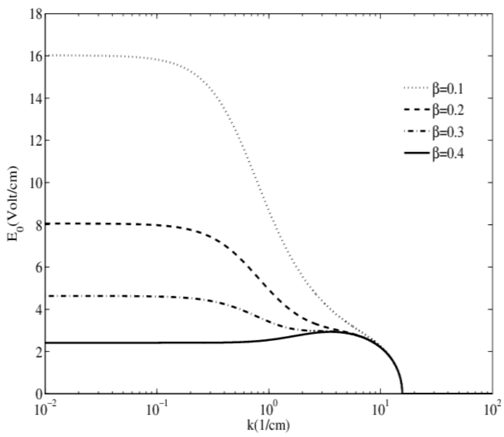

Fig. 6. Neutral curves for the electric field for water-air system at $\hat{\rho} = 0.0012, \hat{\mu} = 0.018, V = 900cm/s$ **for different values of upper different fluid fraction.**

The neutral curves of electric field for the water-air system for various values of upper fluid fraction have been plotted in Fig. 6. The region above the curve represents the stable region while the region below the curve represents the unstable region. It has been observed that on increasing the upper fluid fraction, the stable increases. Therefore, the upper fluid fraction has stabilizing effect on the stability of the system. The effect of relative horizontal velocity on the neutral curves of the electric field has been studied in the Fig. 7. As relative velocity increases, the disturbance will grow faster and system will destabilized. Hence, relative velocity has destabilizing effect on the stability of the system as observed form the Fig. 7.

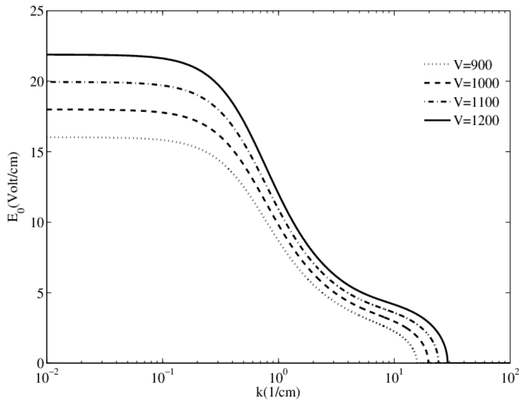

Fig. 7. Neutral curves for the electric field for water-air system at $\hat{\rho} = 0.0012, \hat{\mu} = 0.018, \beta = 0.1$ **for different values of relative velocity.**

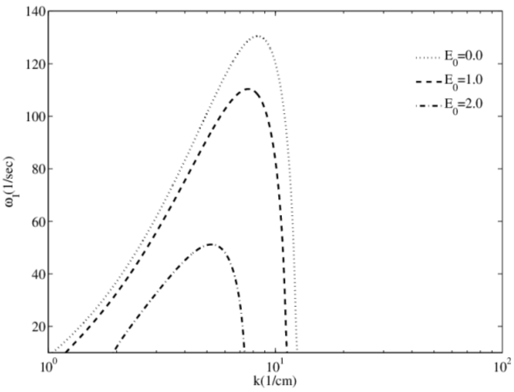

Fig. 8. Growth rate curves for water-air system at $\hat{\rho} = 0.0012, \hat{\mu} = 0.018, \beta = 0.5$ **for different values of electric field.**

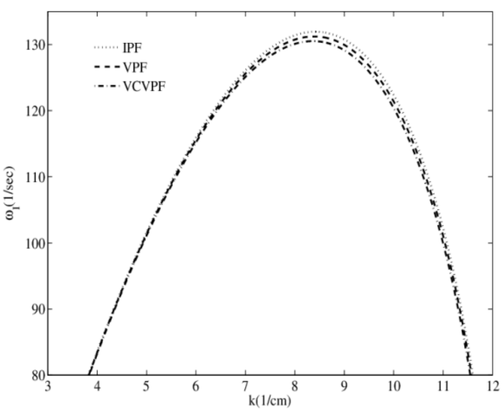

Fig. 9. Comparison between growth rate obtained for VCVPF, VPF and IPF solution when $\hat{\rho} = 0.0012, \hat{\mu} = 0.018, \beta = 0.5$ and $E_0 = 0 volt/cm$ **.**

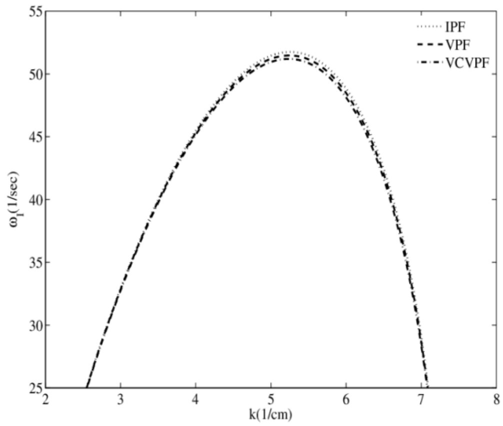

Fig. 10. Comparison between growth rate obtained for VCVPF, VPF and IPF solution when $\hat{\rho} = 0.0012, \hat{\mu} = 0.018, \beta = 0.5$ and $E_0 = 2.0 volt / cm$.

Figure 8 shows the variation of growth rate curves ω_I for the various values of electric field and observed that the growth rate curve decreases as electric field increases. It concludes that electric field has stabilizing effect on the stability of the system.

Figure 9 shows a comparison between the growth rate curves for the water-air system obtained from the VCVPF solution with those obtained from the VPF solution as well as IPF solution. It has been observed that the growth rate in VCVPF solution is lower in comparison with VPF solution as well as IPF solution which indicate that the VCVPF solution is more stable than VPF solution and IPF solution. This occurs mainly because in the VCVPF analysis contains the effect of both shearing stresses as well as normal stresses while in viscous potential flow the effect of tangential stresses is neglected. Inviscid potential flow ignores the contribution of viscosity at all. In other words, we can say that the effect of viscosity is more in VCVPF solution in comparison with the other solutions like viscous potential flow solution or inviscid potential flow solution.

In Fig. 10, the growth rates curves for the water-air system have been compared for the VCVPF solution, VPF solution and IPF solution when the applied electric field $E_0 = 2.0 Volt / cm$. It has been observed that the growth rate curve decreases as electric field increases. It concludes that electric field has stabilizing effect.

7. CONCLUSIONS

A method for calculating a viscous correction of the irrotational pressure has been derived for problems in which the interface of two fluids is involved and the flow of two fluids is irrotational. It is assumed that the viscous corrections of irrotational pressure resolve the discontinuity of the tangential stress and tangential velocity at the interface. This viscous pressure correction is applied to Kelvin- Helmholtz instability in the presence of electric field and compares the growth rate curves with the growth rate curves of viscous potential flow. It is found that the growth rate in VCVPF solution decreases as compared with the VPF solution. It means that VCVPF solution is more stable than the VPF solution. Neutral curves for critical velocity are unaffected with viscous pressure contribution for viscous potential flow solution but VCVPF stabilizes the interface early as compared with the VPF solution. If electric field intensity increases at a constant relative velocity, VCVPF and VPF leads good approximation but if electric field intensity decrease the difference in the growth rates increases. If relative velocity increases at a constant electric field the difference increases and if relative velocity decreases difference also decreases.

ACKNOWLEDGEMENT

Author is thankful to Council of Scientific and Industrial Research (CSIR), New Delhi for their financial support during this work.

REFERENCES

Asthana, R. and G. S. Agrawal (2010). Viscous potential flow analysis of electrohydrodynamic Kelvin-Helmholtz instability with heat and mass transfer. *Int. J. Engineering. Sci.* 48, 1925-1936.

Awasthi, M. K. and G. S. Agrawal (2011). Viscous potential flow analysis of Kelvin-Helmholtz instability of cylindrical interface. *Int. J. App. Math. Comp* 3(2), 131-138.

Awasthi, M. K. and G. S. Agrawal (2011). Viscous contributions to the pressure for the electro-viscous potential flow analysis of capillary instability. *Int. J. Theo. App. Multi. Mech.* 2(2), 130-145.

Awasthi, M. K. and G. S. Agrawal (2011). Viscous contributions to the pressure for the potential flow analysis of magneto-hydrodynamic Kelvin-Helmholtz instability. *Int. J. App. Mech.* 4(1), 1250001 (16 pages).

Chandrasekhar, S. (1981). *Hydrodynamic and Hydromagnetic Stability,* Dover publications, NewYork.

Drazin, P. G. and W. H. Reid (1981) *Hydrodynamic stability.* Cambridge University Press.

Funada, T. and D. D. Joseph (2001). Viscous potential flow analysis of Kelvin-Helmholtz instability in a channel. *J. Fluid Mech* 445, 263-283.

Joseph, D. D., and T. Liao (1994). Potential flow of viscous and viscoelastic fluids. *J. Fluid Mech.* 256, 1-23.

Joseph, D. D., J. Belanger, and G. S. Beavers (1999). Breakup of a liquid drop suddenly exposed to a high- speed airstream. *Int. J. Multiphase Flows* 25, 1263-1303.

Mohamed, A. A. and E. F. Elshehaway (1989). Nonlinear electrohydrodynamic Kelvin-Helmholtz instability: effect of normal field producing surface charge. *Fluid Dynamic Research* 5, 117-133.

Mohamed, A. A., A. R. F. Elhefanwy, and Y. D. Mahmoud (1994). Nonlinear electrohydrodynamic Kelvin-Helmholtz instability with mass and heat transfer: effect of tangential field. *Physica A* 202, 264-1290.

Wang, J., D. D. Joseph, and T. Funada (2005). Pressure Corrections for potential flow analysis of Capillary instability of Viscous Fluids. *J. Fluid* Mechanics 522, 383-394.

Wang, J., D. D. Joseph, and T. Funada (2005). Viscous contributions to the pressure for potential flow analysis of Capillary instability of Viscous Fluids. *Phys. Fluids* 17, 1-12.